ELSEVIER

Biomolecular Engineering
16 (1999) 45–55

Biomolecular Engineering

www.elsevier.com/locate/geneanabioeng

Direct force measurements of the streptavidin–biotin interaction

Joyce Wong [a], Ashutosh Chilkoti [b], Vincent T. Moy [c,*]

[a] *Boston University, Department of Biomedical Engineering, 44 Cummington Street, Boston, MA 02215, USA*
[b] *Duke University, 136 Hudson Hall, Durham, NC 27708-0281, USA*
[c] *Department of Physiology and Biophysics, University of Miami School of Medicine, Miami, FL 33136, USA*

Abstract

The interaction between streptavidin and its ligand, biotin, were studied by direct force measurements. The complimentary approaches of surface force apparatus (SFA) and atomic force microscopy (AFM) were used to elucidate both long-range and short-range adhesive interactions of the streptavidin–biotin interaction. The high spatial resolution of the SFA provided a detailed profile of the intersurface forces of apposing surfaces functionalized with streptavidin and biotin. Measurements obtained by the SFA corresponded to long and intermediate-range forces that are important in determining ligand–receptor association. AFM was used to measure the unbinding force of individual streptavidin–biotin complexes. These measurements revealed the short-range interactions (i.e. hydrophobic and hydrogen bonding forces) that stabilize the intermolecular bond.

Keywords: Streptavidin; Surface force aparatus; Atomic force microscopy

1. Introduction

Living systems make use of both strong and weak chemical interactions [1]. Strong, covalent bonds are naturally suited for static connections; their formation and breakage require enzyme assistance and often stored chemical energy. Once created, the individual covalent bond can withstand the onslaught of thermal agitation. On the other hand, noncovalent weak bonds (i.e. hydrogen bonds and van der Waals interactions) are transient and more suitable for connections that need to be formed and broken rapidly. An individual weak bond has a life expectancy typically several orders of magnitude shorter than the characteristic times associated with most biological processes. However, several weak bonds can combine to form stable, highly specific, intermolecular connections. These molecular recognition interactions, achieved by multiple, individually weak noncovalent bonds between complementary binding partners, underlie the spatial architectures of proteins and nucleic acids, the transient associations formed between enzymes and their substrates, the binding of messenger molecules by their receptors, and the recognition of antigens by antibodies [2].

The dynamical properties of biological systems depend on the reversibility and specificity of the ligand–receptor interactions. These interactions have been studied by thermodynamic analysis and structural approaches such as NMR and X-ray crystallography that characterize systems near equilibrium. Recently, direct force measurements have enabled researchers to investigate properties of systems far from equilibrium and to explore the energy landscape of ligand–receptor interactions. This article is a review of recent developments in this field. The majority of direct force measurement studies of ligand–receptor recognition have focused on the interaction of biotin with avidin/streptavidin [3–9]. The reasons for the popularity of (strept)avidin–biotin as the model ligand–receptor system of choice stem from its unique structural and functional features. These features include the high affinity (dissociation constant of 10^{-13}–10^{-15} M) and specificity of the interaction [10], and the 222 point symmetry of the (strept)avidin homotetramer, which facilitates orientation-specific immobilization of streptavidin via the biotin-binding sites present on one side of the protein, leaving free biotin-binding sites on the opposite face [11–13]. Streptavidin is also extremely stable, as shown by its ability to retain its tertiary structure in the

* Corresponding author. Tel.: +1-305-2436821.
E-mail address: vmoy@mednet.med.miami.edu (V.T. Moy)

1389-0344/99/$ - see front matter
PII: S1050-3862(99)00035-2

presence of a high concentration of sodium dodecyl sulfate, a potent denaturant at elevated temperatures [10,14]. Furthermore, the reactive, carboxy terminus of biotin allows facile attachment of linkers with reactive groups for the immobilization of the ligand to a substrate.

As we will expand on in this review, ligand–receptor interactions involve both long-range and short-range forces. Long and intermediate-range forces are important determinants of ligand–receptor association [15,16] and have been studied with the Surface Force Apparatus (SFA) [17]. The SFA measurements represent the cooperative, ensemble average of interactions between many molecules immobilized on apposing substrates. Inter-surface force is measured as a function of separation, which is obtained independently by an optical interference technique. Short-range forces are involved in specific recognition and stability of ligand–receptor complexes. Direct measurements of short-range binding forces between ligand–receptor complexes were achieved using the Atomic Force Microscope (AFM) [4,6,18–20]. In the AFM experiments, the area over which ligand and receptor interact was limited to the tip of the AFM probe. This restricted the interaction to a small number of molecules and consequently, the rupture force of a single complex was frequently recorded. Another feature of the AFM is its ability to investigate the local inhomogeneity of the substrate in the affinity imaging mode [21]. Together, the SFA and AFM experiments furnish complementary information that have been used to develop a more comprehensive description of the interaction forces between ligand–receptor complexes. This review focuses on results obtained with the SFA [17,22] and AFM [23,24]. Other techniques including micropipette aspiration measurements [25,26], optical tweezers [27], magnetic torsion measurements [28], and shear flow measurements [29] while undeniably useful in force measurements are not covered in this review.

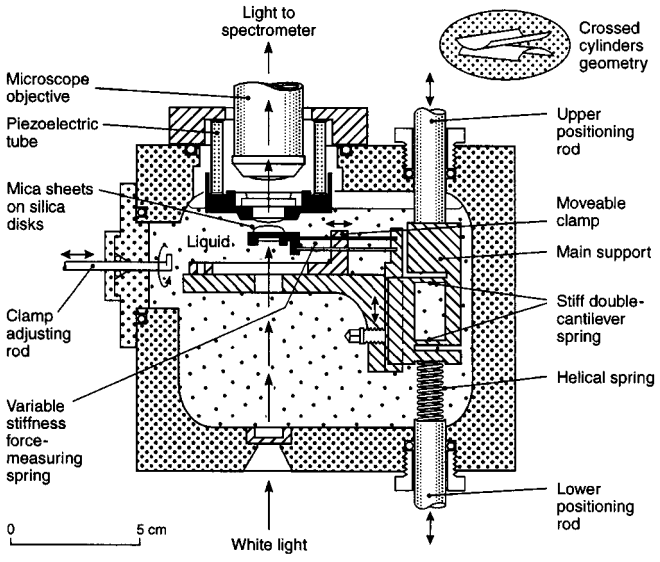

Fig. 1. The design of a surface forces apparatus (SFA). The forces between two surfaces can be measured with a sensitivity of a few millidynes (10 nN) and a distance resolution of 1 Å. One surface is rigidly mounted at the end of a piezoelectric crystal tube while the other surface is suspended at the end of a force-measuring spring. The stiffness of the force-measuring spring can be adjusted during an experiment by a factor of up to 10 000 thus enabling forces of greatly differing magnitudes to be measured. Syringe ports (not shown) allow the solution to be changed during an experiment if necessary.

2. Streptavidin–biotin interaction assayed by the surface forces apparatus (SFA)

The SFA allows one to directly measure the interaction forces between surfaces at the molecular level and, independently and unambiguously, the geometry and absolute separation distance between two surfaces. Fig. 1 shows the central components of the experimental setup [30]. The substrates consist of two transparent back-silvered mica sheets of equal thickness glued onto cylindrically curved silica disks. Mica is used because it can be easily cleaved to be atomically smooth over large areas ($\approx$ a few cm^2). The separation distance between the two surfaces can be controlled over a range of 5 mm with a resolution of 1 Å by a four-stage mechanism of increasing sensitivity. The separation between the surfaces can be measured to ± 1 Å by monitoring the movement of the multiple beam interference fringes known as Fringes of Equal Chromatic Order (FECO) produced when white light passes normally through the two surfaces. When strongly attractive forces are measured, mechanical instabilities can occur causing the surfaces to jump from one stable position to another. Instabilities occur whenever the gradient of the force exceeds the spring stiffness.

Fig. 2 is a schematic of the streptavidin- and biotin-coated surfaces prepared in a similar fashion as the procedures of Ringsdorf et al. [31]. Planar lipid bilayers are deposited onto both mica substrates via the Langmuir–Blodgett (LB) technique. The LB technique allows one to deposit the phospholipid molecules at a controlled surface pressure, and hence control the packing or fluidity of the monolayer. The outer monolayer contains a controllable fraction of biotinylated phospholipids to which streptavidin adsorbs via self-assembly (Fig. 2, top).

Structural information gained by microscopic or scattering techniques provides invaluable insight for interpreting data from direct force measurements. For the system illustrated in Fig. 2, Ringsdorf et al. [31] as well as other groups showed that an oriented streptavidin monolayer (two-dimensional crystals) forms underneath a monolayer of biotinylated phospholipids at the air-water interface as determined by fluorescence

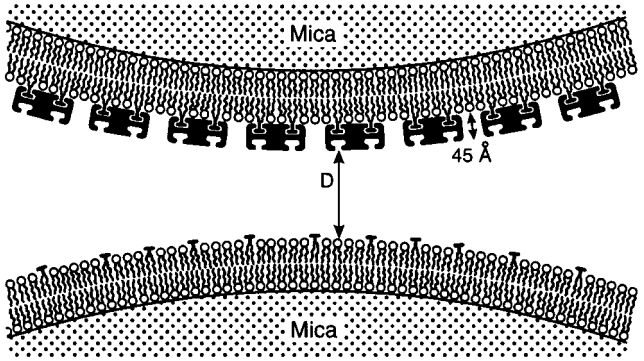

Fig. 2. Schematic representation of a streptavidin-coated surface and a biotin-coated surface. The streptavidin is physisorbed to a biotinylated phospholipid bilayer, which is in turn physisorbed to the underlying mica surface. The tetravalent nature of streptavidin allows it to be anchored to the bilayer, leaving two empty sites for interaction with the apposing biotinylated surface. The silica disks supporting the mica substrates are in crossed cylinder geometry, and for two crossed cylinders with 1 cm radii of curvature, the effective contact area is approximately 100 μm^2. The magnitude of this contact area scales with the geometric average radius R; thus, data are always reported as F/R, the force normalized by the average radius of curvature.

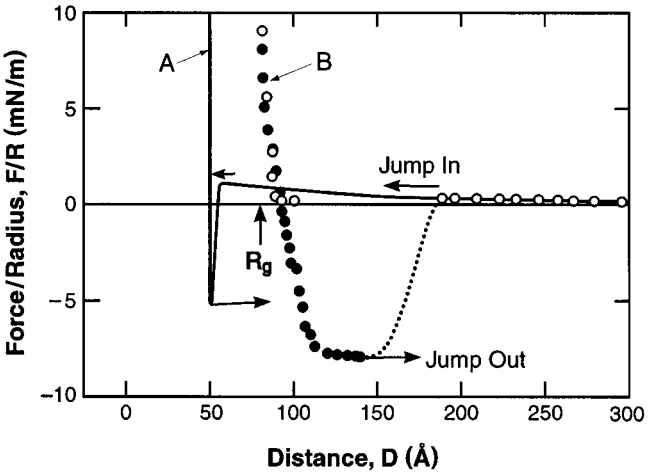

Fig. 3. (A) Biotin–streptavidin interaction (solid curve) for schematic in Fig. 2. (B) Tethered ligand–receptor interaction potential, including approach (open circles) and separation (closed circles) of surfaces.

and electron microscopy. In addition, AFM studies [32] showed that streptavidin can adsorb to planar substrate-supported bilayers. Such well-defined surfaces in which the molecular dimensions are known for each of the components are ideal for surface force measurements.

A representative SFA force curve between streptavidin and biotin [3,22] is shown in Fig. 3 (solid curve). Under the experimental conditions (pH 7.2), both streptavidin and the biotinylated surface are negatively charged and hence there is a long-range electrostatic repulsion. Further verification of the double-layer force was shown when the long-range interaction became attractive by altering the streptavidin surface potential from net negative to net positive by changing the pH from 7.2 to 6.0 [17]. As the surfaces continue to approach each other ($\approx$10–20 Å separation), repulsive steric interactions attributed to the time-dependent reorientation of the biotin head groups which precede biotin–streptavidin binding were found to be dependent on the rate of approach of the apposing surfaces [17], i.e. the steric repulsion is not observed if the surfaces are approached at a much slower rate. Thus, the time-scale of the interaction is important in that the rates of approach and separation and application of an external force all play a role in altering the interaction. At short distances less than 5 Å, the biotins lock into the streptavidin binding sites and very strong adhesion due to the specific binding is observed [3,22] (Fig. 3, solid curve).

2.1. Probing dynamics of tethered-biotin interaction with streptavidin with SFA

Wong et al. [33] investigated the effect of attaching the biotin to the end of a flexible polymer tether on the streptavidin–biotin interaction potential. In many biotechnological applications designed for selective targeting, the ligand is often tethered to the surface. For example, in liposomes decorated with polyethylene glycol (PEG) chains which serve as a steric stabilizer in order to dramatically increase circulation times from minutes to days, the targeting moiety is attached at the extremity of a PEG [34].

Fig. 4 is a schematic of the surfaces used to probe the interaction of tethered-biotin with streptavidin. Fig. 3 shows the interaction profile for both the tethered (circles) and untethered biotin (solid line). At large distances the same non-specific DLVO interaction as determined in the case when the biotin ligand is attached via short spacer is measured. The most surprising result, however, was the finding that the biotin ends locked into the opposing streptavidin binding site at a

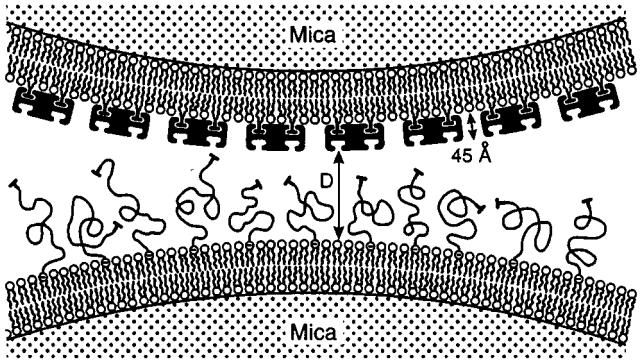

Fig. 4. Schematic of the tethered ligand–receptor surfaces. The surfaces are the same as in Fig. 2 except the ligands are now tethered to the surface via a polyethylene glycol chain (2000 MW) which in turn is covalently attached to a phospholipid headgroup.

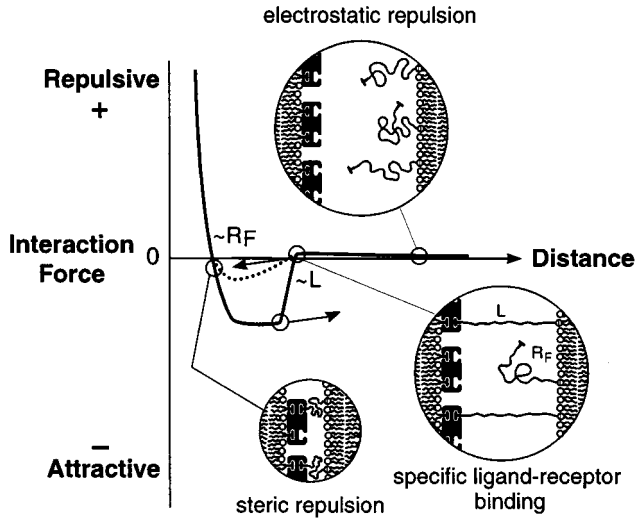

Fig. 5. Total force profile of tethered ligand–receptor interaction.

distance much larger than the radius of gyration (R_g) of the polymer (PEG-2000) tether. Kuhl et al. [35] showed that for two symmetric surfaces containing polyethylene glycol tethers of the same molecular weight, the deviation from the electrostatic repulsion due to the polymer steric interaction occurred at approximately 2Rg. What was observed in the tethered biotin and streptavidin system, however, was that the jump-in occurred at a distance near the fully-extended length (70% extension) of the polymer! This observation suggests that the end of the polymer chain, or biotin molecule, freely sampled all conformations up to full extension. Thus, when the biotin end came within 5Å of its streptavidin binding site, the specific, short-range interaction locked in. Fig. 5 illustrates the total force profile of the tethered ligand-receptor interaction potential. These measurements illustrate the power of the SFA technique and demonstrate that one can quantitatively and directly study specific biomolecular interactions at the molecular level and the dynamics 'real time'.

3. Streptavidin–biotin interaction assayed by the atomic force microscope (AFM)

Whereas force versus separation curves derived from the SFA provide a direct measure of long-range interactions between two surfaces, the AFM provides access to the short-range forces that stabilize the individual (strept)avidin–biotin complex. Fig. 6A shows the central components of an experimental setup in the AFM force measurements [5]. A tip (20 nm in diameter) protruding from a 'V' shaped cantilever mounted on an AFM (Fig. 6B) and an agarose bead (≈ 100 μm in diameter) provide the two apposing surfaces that are coated with the binding partners to be tested (Fig. 6C). The attachment of the test molecules to their respective substrates is supported by forces larger than those developed at the bond under test. Biotin is covalently linked (by an ester bond to the carboxyl group) to both the agarose of the bead and to a layer of bovine serum albumin (BSA) that coats the cantilever tip. To form a (strept)avidin-functionalized tip, the biotin-precoated tip is saturated with (strept)avidin, which is a homo-tetramer with 4 binding sites for biotin (Fig. 7). Some of these binding sites will anchor the avidin to the tip, and some will remain free for reaction with the agarose-bonded biotin.

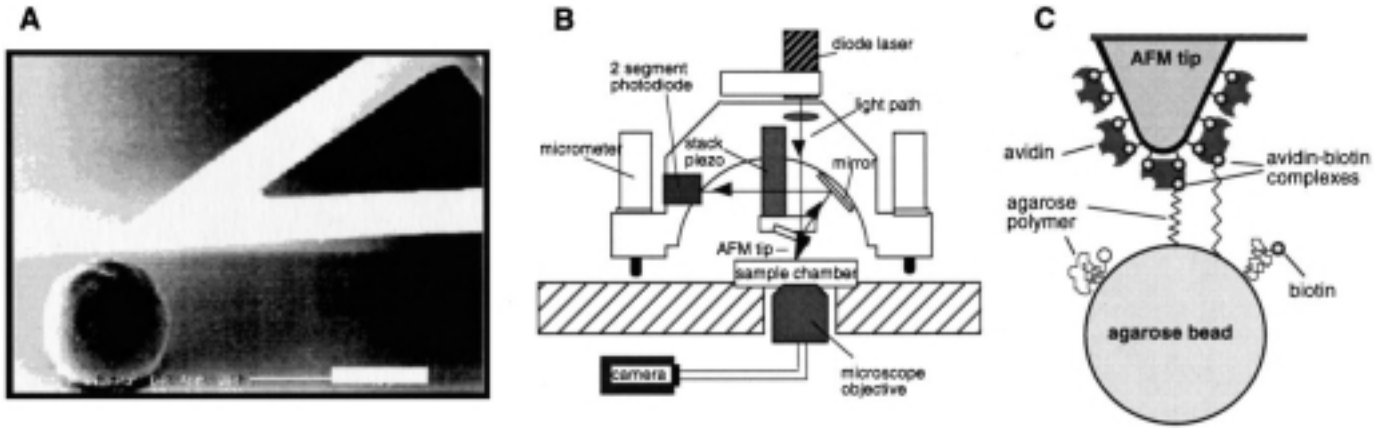

Fig. 6. (A) Electron micrograph of an AFM cantilever and an agarose bead (bar = 50 μm). (B) The design of an atomic force microscope (AFM) modified for force measurements. The tip-cantilever is mounted on a stacked piezoelectric translator, which generates the vertical movements of the cantilever. The precision of the vertical displacement is less than 1 Å. The deflections of the tip-cantilever by forces acting between the tip and the sample are monitored optically. A focused laser beam from a diode laser is reflected from the upper surface of the cantilever to a fixed mirror and onto a 2-segment photodiode. The deflection of the cantilever is obtained by measuring the difference between the photo-current of the two segments. (C) Schematic representation of the interaction between an AFM tip, functionalized with avidin molecules, and a biotin-dervatized agarose bead (not drawn to scale). The biotin molecules are covalently coupled to the bead via molecular agarose filaments with an estimated extended length of over 100 nm and spring constant of 2 mN/m. During the withdrawal of the AFM tip, the agarose filament stretches, permitting the tension across the avidin-biotin complex to increase gradually.

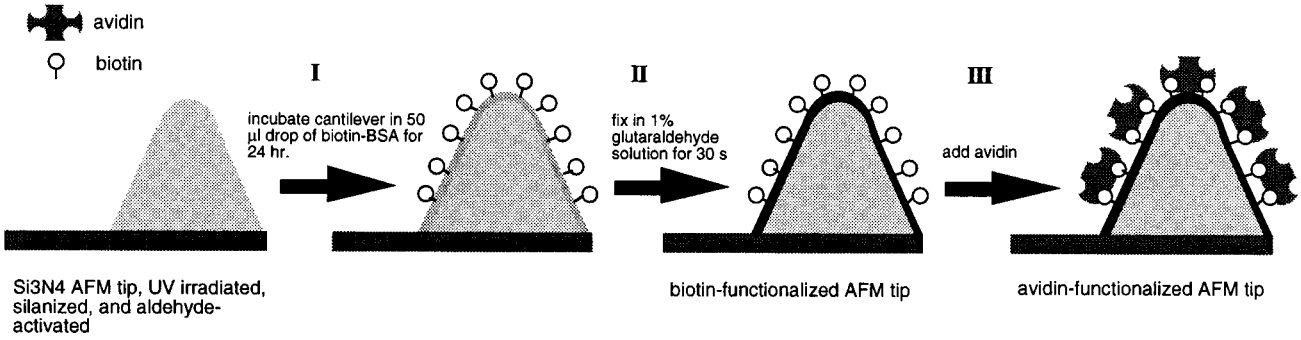

Fig. 7. Functionalization of AFM tip with avidin.

A representative AFM force scan measurement carried out with the functionalized surfaces is shown in Fig. 8. During the approach phase of the recording cycle, the AFM tip is lowered onto the biotin sample. No interaction was detected between the surfaces until surfaces made contact. Bonds formed between avidin and biotin force the cantilever to bend downward while the cantilever base is lifted upward during retraction. The force on the avidin–biotin bonds is increased gradually by the withdrawal of the cantilever until the bonds fail. The sharp vertical transition in the retraction trace corresponds to the separation of surface contact [36–38]. The magnitude of the vertical transition is the adhesive strength of the avidin–biotin interactions. The number of avidin–biotin complexes involved in this particular measurement is estimated to be about 100. This large number is possible even though contact is limited to the apex of the AFM tip. Since the agarose bead is elastic, the contact surface can be enlarged when the tip is indented into the bead, thus permitting a large number of molecules to interact.

Several controlled experiments were made to confirm that the adhesion detected in the force measurement was due to the specific interaction between avidin and biotin. First, excess avidin (but not serum albumin) or biotin added to the solution completely eliminated the adhesive force (Fig. 8B). Second, the approach/withdrawal cycle could be repeated many times with reproducible results (Fig. 9). This demonstrated that the avidin–biotin bond was ruptured during the force measurement. If, for instance, the molecular linkages formed between the surfaces were broken at either the covalent ester bonds or between avidin subunits, these links, unlike the reversible avidin-biotin bond, would not have readily re-formed when the tip and bead were re-approached in subsequent trials, and a rapid decline of adhesive force would have occurred with subsequent trials. A decline was actually observed during the first 100 cycles in the experiment of Fig. 9, suggesting some initial irreversibility, but then a stable plateau was maintained in the subsequent 400 trials (and extending to 5000 trials in some experiments).

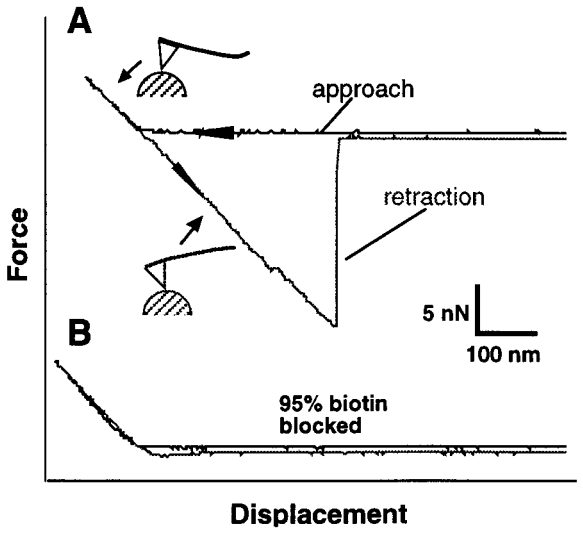

Fig. 8. (A) AFM force versus displacement curve curves of avidin-functionalized AFM tip and biotin-dervatized bead, and (B) after the addition of soluble avidin. Measurements were carried out in phosphate buffered saline at 18°C. The deflection of the cantilever was measured on approach and retraction of the cantilever.

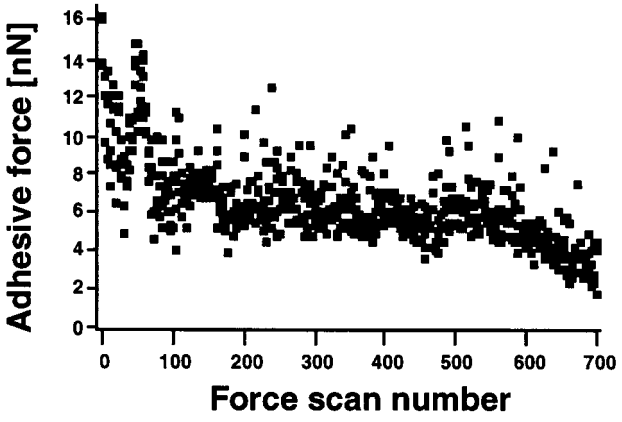

Fig. 9. Stability of avidin-functionalized AFM tip. The activity of the functionalized tip was assayed by its adhesion to a biotin-derivatized agarose bead in successive force measurements. The force scan number refers to a measurement within the series.

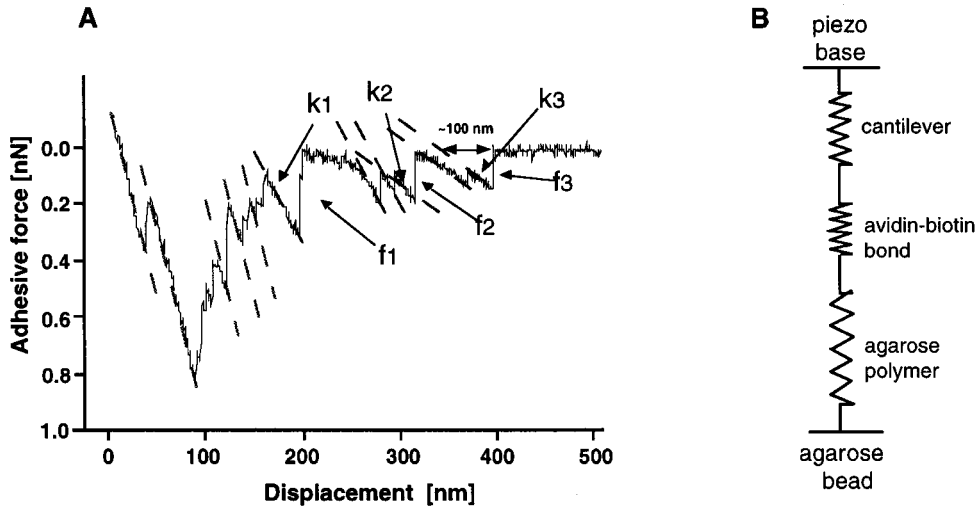

Fig. 10. (A) AFM force versus displacement profile. Under conditions where a small number of avidin–biotin complexes are permitted to form, the breakage of individual complexes can be detected. As shown, the separation of the avidin-functionalized AFM tip from the biotin-functionalized agarose occurs in a series of steps in which one to six complexes are ruptured. f3 denotes the rupture force of the last complex in the measurement. The rupture forces (f1 and f2) of prior events are an integer multiple of f3; f1 = 2f3 and f2 = f3. k1, k2 and k3 denote the observed spring constants of the system prior to the rupture of the designated bond(s). (B) Representation of elastic elements in the AFM force measurement. Approximate spring constant values of the cantilever, avidin–biotin bond, and agarose polymer are 60, 2, and 200 mN/m, respectively.

3.1. Rupture force of individual avidin–biotin complexes

The interaction between the avidin tip and biotin bead could be reduced significantly to the point where on average only a small number of avidin–biotin bonds were formed by the addition of an excess amount of soluble avidin to block the biotin molecules on the bead. The retraction trace of a force measurement carried out under these conditions is presented in Fig. 10A. Here, the gradual withdrawal of the cantilever was associated with multiple jumps in both the force and the spring constant (slope of the force-length relationship), as if a small number of avidin–biotin bridges were broken sequentially. (The displacement plotted in Fig. 10A as well as in Fig. 8 refers to the base of the cantilever, not the AFM tip which remained in contact with the surface until all bonds are broken. This displacement reflects the bend of the cantilever, the stretching of avidin-biotin bonds, and the elongation of the agarose filament that anchors biotin to the bead (as illustrated in Fig. 10B). The overall compliance of this series of 'springs' is determined mainly by the elasticity of the agarose polymer. The tension (force) is the same along the entire chain and is measured by the deflection of the cantilever.) Over the first 150 nm of displacement (using the position of zero force as reference), the slope of the continuous force changes (dashed lines in Fig. 10A) was steep and not detectably reduced over a number of sudden decreases in force. This would be expected if only a small fraction of the adhesion was broken in each force jump. In fact, changes in the spring constant only occurred at displacements at which the adhesion force had dropped substantially. Between 200 and 300 nm of displacement, there was an interval of small slope and zero tension, as if following the preceding force jump there was slack in the remaining bridges. Three force jumps (f1, f2 and f3) are labeled in Fig. 10A. The amplitudes of these force jumps are 320, 160 and 160 pN, suggesting that these transitions correspond to the breakage of two parallel avidin-biotin bonds, followed by the sequential breakage of two single bonds.

A histogram of measured force jumps (Fig. 11A) obtained under conditions that allowed only a few avidin-biotin bonds to form revealed several peaks at integer multiples of 160 pN, the signature of a quantal behavior [6]. An autocorrelation analysis was performed on the force histogram to test this periodicity statistically. Based on this analysis, it was concluded that the value of the first peak was the rupture force of a single avidin–biotin complex, and the values of the subsequent peaks to multiples of this interaction. Analogous experiments done with avidin and iminobiotin, a biotin analogue, under the same experimental conditions, also yielded a quantal distribution of force increments, but the increments were approximately 85 pN (Fig. 11B). The force quanta thus appear to follow the pattern of binding affinity, as avidin binds biotin much more strongly than iminobiotin [6]. The unitary rupture force of three other avidin-biotin analogs have also been measured [39]. The rupture force in this series of protein–ligand pairs varies between 85 and 255 pN. Altogether, these experiments demonstrate that the

AFM assay can resolve forces associated with the specific avidin–biotin interaction at the level of a single molecular pair.

3.2. Relationship between ligand-binding thermodynamics and rupture forces

In a complementary AFM study, Chilkoti et al. [8] measured the biotin-interaction forces for site-directed mutants of recombinant core streptavidin, which displayed a range of biotin-binding thermodynamic and kinetic properties. They further correlated the measured forces for the various mutants with their biotin-binding equilibrium and activation thermodynamic parameters. The primary advantage of this experimental approach lies in the systematic variation of ligand-binding parameters within a single protein–ligand system by precise, molecular alterations in the active site of the protein. Subsequent interpretation of the AFM-measured interaction forces can then be rationally approached within the context of the independently measured energetics of ligand binding and dissociation.

The X-ray crystal structure of apostreptavidin and biotin-bound wild-type (WT) streptavidin provides detailed molecular-level structural information underlying the streptavidin–biotin interaction, which includes extensive hydrogen-bonding, prominent aromatic contacts, and conformational changes associated with flexible loop closure and quaternary structural alterations [11–13,40–42]. Additionally, computational studies have suggested that the four Trp residues in contact with biotin contribute significantly to the large equilibrium free energy of biotin association [43,44]. Motivated by these studies, site-directed mutagenesis was used to alter Trp79, Trp108, and Trp120 to Phe or Ala residues at the biotin-binding site [42]. These Trp mutants display a range of equilibrium and activation thermodynamic properties, including an interesting case where the equilibrium and activation thermodynamic properties are altered in opposite directions [8,41,42], allowing their contributions to the AFM interaction force to be delineated.

The specific force of biotin-detachment was measured by AFM for the various mutants, and varied from 90 to 400 pN (Table 1). The average nonspecific force for all experiments was 105 ± 60 pN. These results, particularly for wild-type (WT) streptavidin agree well with previous measurements by other groups [4,39]. The discrimination of mutants based on the measured force of detachment clearly demonstrated that AFM can be used to characterize the differential biotin interaction forces arising from site-specific, single residue alterations in the biotin-binding site of streptavidin. The independently measured thermodynamic difference parameters for the site-directed Trp mutants ($\Delta\Delta X = \Delta X(\text{mutant}) - \Delta X(\text{WT})$ where ΔX is the equilibrium or activation thermodynamic parameter of interest) were also compared with a similarly derived differential force parameter ($\Delta\Delta F = \Delta F(\text{mutant}) - \Delta F(\text{WT})$ where $\Delta F =$ specific force of interaction for the mutant or WT streptavidin). No correlation ($R^2 < 0.8$) was observed between either $\Delta\Delta G^{\circ}$ or $\Delta\Delta G^{\neq}$ and $\Delta\Delta F$ for the different streptavidin mutants (results not shown).

However, both the biotin-binding equilibrium difference enthalpy ($\Delta\Delta H^{\circ}$) and the difference activation enthalpic barrier to biotin dissociation ($\Delta\Delta H^{\neq}$) correlated with $\Delta\Delta F$ ($R^2 > 0.94$). These results, albeit based on a limited set of mutants, reveal that the AFM-measured interaction forces correlate with enthalpic parameters and not with free energy. These results suggest that the force measurements directly probe the internal energy associated with the bond-breaking processes and are insensitive to entropy change associated with ligand dissociation (which arise from changes in

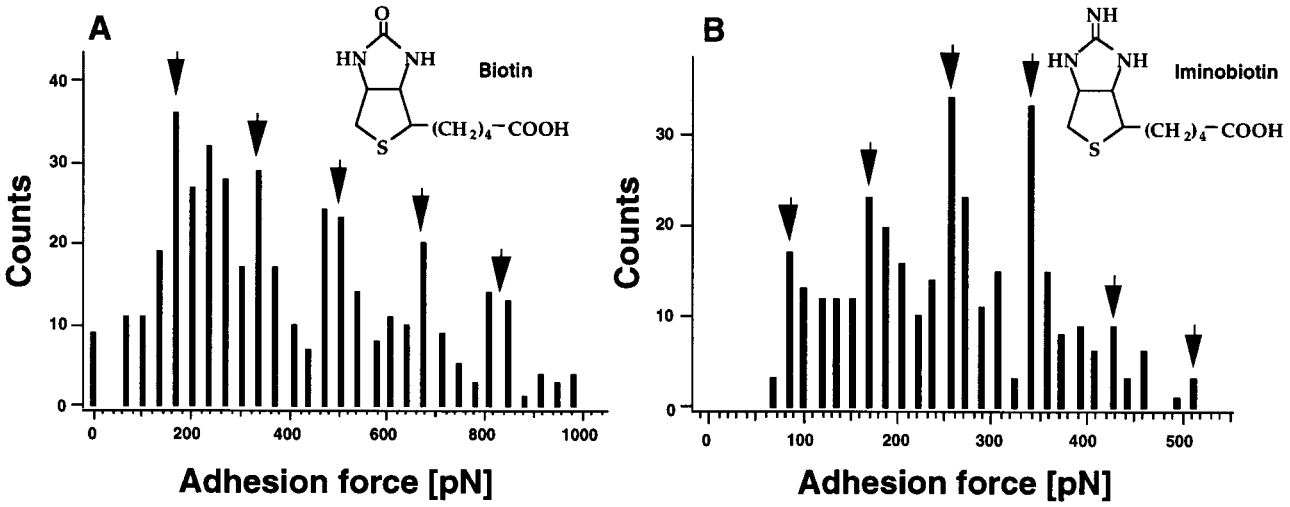

Fig. 11. Histograms of (A) biotin-avidin and (B) iminobiotin–avidin rupture forces. The arrows point to the locations of peaks in the histograms as determined by autocorrelation analysis.

Table 1
Summary of the AFM-measured forces and energetic parameters for the interaction of WT streptavidin and Trp site-directed mutants with biotin at 298 K[a]

Protein	Specific force (pN) [ΔF]	ΔΔF (pN)	ΔΔG°	ΔΔH°	$\Delta\Delta G^{\neq}$	$\Delta\Delta H^{\neq}$
WT streptavidin	(a) 253 ± 20 (b) 393 ± 10[b]	0	ΔG° = −18.3 ΔΔG° = 0	ΔH° = −24.5 ± 0.5 ΔΔH° = 0	$\Delta G^{\neq}$ = 24.4 ± 2.4b $\Delta\Delta G^{\neq} = 0$	$\Delta H^{\neq} = 32 \pm 2.1$ $\Delta\Delta H^{\neq} = 0$
W79A	(a) 158 ± 17 (b) 332 ± 31	−95 −61	+7.6	+6.0	nd[c]	nd
W79F	(a) 294 ± 10 (b) 439 ± 11	+41 +46	0.8	−1.5	−1.1	+2.9
W108F	(b) 443 ± 33	+50	0.5	+1.0	−1.7	+4.5
W120A	(b) 257 ± 28	−300	+8.8	+11.7	nd	nd
W120F	(b) 92 ± 19	−136	2.7	+5.1	−2.5	−3.5

[a] The specific force of detachment (ΔF) is the difference between the total measured force of interaction and the residual force measured upon blocking biotin-binding sites by free biotin present in excess in the imaging buffer. The difference force parameterΔΔF is ΔF(mutant) − ΔF(WT). The AFM data were obtained by averaging the results from 100 force versus displacement curves for each sample. The biotin-binding equilibrium thermodynamic difference parameters (free energy:ΔΔG°; enthalpy:ΔΔH°) and activation thermodynamic difference parameters ((free energy:$\Delta\Delta G^{\neq}$; enthalpy:$\Delta\Delta H^{\neq}$) of streptavidin–biotin dissociation are also reported. All thermodynamic parameters are in kcal mol^{-1}. ΔΔX = ΔX(mutant) − ΔX(WT) whereΔX is a thermodynamic parameter of interest.

[b] (a) and (b) refer to two independent experiments performed with different tips.

[c] nd: not determined. The biotin-dissociation kinetics of these mutants are too rapid to allow determination of the activation thermodynamic parameters by the methods utilized for the other mutants in this study.

the translational and rotational degrees of freedom of ligand and protein, dilution effects, changes in protein conformation, and solvent reorganization) [45,46].

However, there was an important exception to this overall trend for one mutant, W108F, which allowed the apparent correlation of ΔΔF with both $\Delta\Delta H^{\circ}$ and $\Delta\Delta H^{\neq}$ to be examined in greater detail. The activation enthalpy for dissociation ($\Delta H^{\neq}$) and the equilibrium biotin-binding enthalpy (ΔH°) for the W108F mutant are altered in opposite directions, relative to WT streptavidin. The larger interaction force for W108F, relative to WT streptavidin (ΔΔF = + 50 pN), positively correlated with the increased activation enthalpic barrier ($\Delta\Delta H^{\neq} = +4.5$ kcal mol^{-1}) but not with the decreased equilibrium biotin-binding enthalpy ($\Delta\Delta H^{\circ} = +1.0$ kcal mol^{-1}) (Table 1).

This result can be understood by examining the origins of the thermodynamic alterations ensuing from a binding-site mutation. There are two limiting cases, and the thermodynamic effects of a specific mutation is in general some combination of these two effects. The first limiting case, shown in Fig. 12B, is when the mutation, relative to WT protein (Fig. 12A), solely alters the enthalpy of the protein-ligand complex with no effect on the transition state. For all the Trp mutants with the notable exception of W108F, the mutation has the effect of decreasing the enthalpy of the protein–ligand complex. This change is then equally manifest in a decreased activation barrier to dissociation. Therefore for mutations that can be described by this limiting case, $\Delta\Delta H^{\circ}$ and $\Delta\Delta H^{\neq}$ are correlated and the relationship between the differential force of interaction, ΔΔF and alterations in the equilibrium enthalpy and activation enthalpic barriers cannot be easily separated.

The second, converse case is when the mutation only affects the transition state, leaving unperturbed the protein–ligand complex (Fig. 12C). The W108F mutation is illuminating within this context because it corresponds to the second limiting case: *this mutation largely affects the enthalpy of the transition state*. The increased activation enthalpic barrier of + 4.5 kcal mol^{-1} for W108F, relative to WT streptavidin, is dominated by the + 5.5 kcal mol^{-1} destabilization of the transition state ($\Delta\Delta H^{TS} = +5.5$ kcal mol^{-1}), with a small, and opposing change in $\Delta\Delta H^{\circ}$ (+ 1 kcal mol^{-1}). The larger force measured for W108F, relative to WT streptavidin (ΔΔF = + 50 pN) correlates with the increased activation enthalpic barrier ($\Delta\Delta H^{\neq} = +4.5$ kcal mol^{-1}) but not with the decreased equilibrium binding enthalpy of

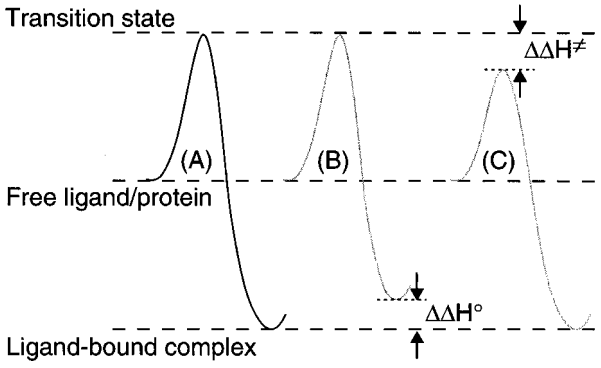

Fig. 12. Schematic of ligand-binding enthalpy diagram of: (A) WT protein; (B) site-directed mutant with altered equilibrium enthalpy of protein-ligand binding, and no effect on the transition state; and (C) site-directed mutant with altered activation enthalpy dissociation, with no effect on the equilibrium enthalpy of protein–ligand binding. The energy diagram is referenced to the unbound protein and free ligand as zero. ΔΔH is the difference enthalpy defined as ΔH(mutant) − ΔH(WT), superscripts ° and ≠ refer to ligand-bound equilibrium and activation barrier for dissociation, respectively.

W108F ($\Delta\Delta H^{o} = +1$ kcal mol^{-1}). These results suggest that the AFM detachment process for this mutant follows the enthalpic barrier to dissociation, and that the apparent correlation of $\Delta\Delta F^{o}$ with $\Delta\Delta H^{o}$ for all the other mutants arises because changes in the enthalpy level of the ligand-bound state, i.e. the protein–ligand complex, are folded into the magnitude of the activation enthalpy.

4. Discussion

4.1. Energetics of tethered receptor–ligand interaction

The results from the SFA tethered receptor–ligand experiments demonstrate that the total energy of the systems is controlled by *both* the ligand-receptor bond energy and the length of the tether. The polymer chain dynamics of the tethered receptor may be a general means of controlling the effective receptor–ligand on-rate process independently from the specific ligand–receptor affinity in biological interactions. The question then becomes if this is reasonable from an energetic standpoint. One needs to estimate the energy needed to stretch a polymer chain to near full extension. Theories of end-grafted polymer chains have predicted that the free chain ends are, on average, located at a distance of 0.7 $R_g$from the anchoring surface. However, thermal fluctuations allow the polymer to sample all possible configurations ranging from a random-coil to nearly fully extended state. The typical exploration time, τ, for a particle diffusing in an external potential, $E_{ext}(D)$, (in our case, the time it takes for a tethered biotin to find its binding site) is given by Kramers' equation:

$$\tau(D) = \tau_0 \exp[E_{ext}(D)/kT] \quad (1)$$

where k is the Boltzmann constant and T is temperature. The basic attempt rate for a chain to reach near full extension, τ_0, is the Zimm time

$$\tau_0 \approx \frac{\eta R_g^3}{kT} \approx 10^{-8}\text{s} \quad (2)$$

where η is the viscosity of water. A rough estimate of $E_{ext}(D)$ for $D > R_g$ is to model the polymer chain as a spring with a parabolic potential:

$$E_{ext}(D) = \frac{(D/R_g)^2 kT}{2} \quad (3)$$

For PEG (2000 MW), $D/R_g = 5$, and Eqs. (3) and (2) and Eq. (1) give τ in the millisecond range which is consistent with the observation of a rapid locking-on.

However, a polymer does not strictly follow a parabolic potential. A more refined Monte-Carlo simulation of a single polymer chain (manuscript in preparation) shows that a polymer chain of 45 monomer units (2000 MW) is able to reach 70% extension in 1 s, which is of the time-scale of our measurements. Thus, the measured tethered interaction potential and its dynamics can still be modeled using standard theories of polymer and colloidal interactions.

4.2. Separation of surfaces: ligand–receptor bond failure versus membrane failure

In contrast to the AFM experiments where the streptavidin-biotin bond is ruptured, in SFA experiments lipid pull-out was observed. In the SFA experiments, streptavidin and biotin were immobilized onto planar lipid bilayers which leads to competing failure mechanisms: [1] ligand-receptor bond failure or [2] membrane failure. When lipids are extracted from a membrane, the energy to pull out a lipid from a bilayer is 16 kT. Assuming that potential changes linearly over the entire length of the lipid (in our case, 28 Å), the force needed to extract the lipid from the membrane is 23 pN [3]. On the other hand, the streptavidin–biotin bond energy is 31 kT, and its effective length is approximately 9 Å giving a force of 140 pN. Thus, for both the PEG-tethered biotinylated lipid and the biotinylated lipid, a much lower force is needed to pull out lipids than to break individual streptavidin–biotin bonds. In addition, significant hysteresis in the force curve giving decreased adhesion on subsequent approach of the surfaces as well as an increase in the layer thickness indicates that the lipids are being pulled out of the membrane and remain on the surface coated with streptavidin rather than streptavidin–biotin bond breakage. This has been tested for a series of biotin-analogs with affinities ranging over 10 orders of magnitude [47] in which for sufficiently weak biotin-analogs, the receptor–ligand bond was the weaker link and the expected changeover in the bond failure mechanism was observed.

4.3. Theoretical approaches: dynamic strength of ligand–receptor interactions

Close to physiological conditions, the dissociation of the avidin–biotin complex is slow, and involves crossing an activation energy barrier of more than 20 kcal/mol. As demonstrated by the AFM measurement, the dissociation time can be reduced significantly by the application of an external force. Theoretically, the external force causes a distortion in the pair potential of the streptavidin-biotin complex that reduces the lifetime of the bond. Bell argued that the activation energy of biochemical bond is reduced by $f^{\circ}\gamma$, where f° is the applied force and γ is a displacement parameter that characterizes the interaction [48,49]. The lifetime of the complex is then: $\tau = \tau_o \exp[(E_o\text{-}f^{\circ}\gamma)/kT]$, where E_o is the intrinsic dissociation energy barrier and τ_o is a phenomenological prefactor. More recently, Evans ex-

tended the Bell model to consider the effects of viscous damping and hydrodynamics on the forced dissociation of biochemical bonds [50]. Applying Kramers' theory for reaction kinetics in condensed liquid to the bond dissociation under external force [51], Evans and Ritchie showed that the unbinding force of biochemical bonds progresses through three regimes of loading rate. In the slow-loading regime that characterized many physiological processes and the AFM experiments, the unbinding force increased as a weak power of the loading rate. At intermediate loading rates, the strength of the bond increased as the logarithm of the loading rate. In the ultrafast regime that approaches the regime of molecular dynamic (MD) calculations, the loading force overwhelmed the bonding potential and only friction remained to retard dissociation.

While the theoretical models have provided a key link between the AFM unbinding force and loading rate, many questions regarding the energetics and reaction trajectories remain to be elucidated. MD simulation has provided some insight into the unbinding pathway of the streptavidin-biotin complex. Grubmüller et al. [52] simulated the forced unbinding of biotin from the streptavidin monomer in a water sphere. The dissociation of the complex was induced by the displacement of a spring potential assigned to the carboxyl group of biotin. The trajectory of the restoring force revealed an overall increase of force, followed by a drop to the baseline as separation was achieved. The force profile also revealed several jumps that coincided with the separation of individual hydrogen bonds between the binding pocket wall and biotin. In addition, the simulation identified water in playing a prominent role throughout the dissociation process by bridging the interactions between biotin and the hydrophilic residues in the binding pocket.

In a separate MD study, Izrailev et al. [53] examined the unbinding of biotin from the avidin tetramer in the absence of water. The ground state of the avidin–biotin complex is stabilized by hydrogen bonds formed between the head group of biotin and polar residues in the binding pocket, most notably Asn12 and Tyr33, and to an lesser extent, by van der Waals interactions with Phe79 and Trp97. With increasing applied force, the system undergoes transitions into 2 well-defined intermediate states in which positions of biotin remained relatively constant with increased force application. The first intermediate state is stabilized by hydrogen bonds involving Thr35 and Ser16, and vdw interactions involving Trp110 and Trp70. After the biotin is extracted from the binding pocket, it still remained associated with the avidin via interaction between the biotin head group and the avidin residues outside the pocket, including those from the 3–4 loop of an adjacent subunit.

It should be noted that the MD calculations were carried out with separation velocities that were at least six orders of magnitude higher than the fastest velocity that was tested experimentally. While a direct comparison of the AFM experiments and MD simulations may not be appropriate, the MD calculations raise the possibility that the unbinding of the streptavidin–biotin complex may involve transitions between intermediate states before total separation occur. The dissociation of a complex that involves series of intermediates may have unbinding forces significantly lower than complexes that undergo a cooperative dissociation of all their intermolecular bonds. Future experiments that investigate the kinetics of the stressed streptavidin–biotin bond may provide more direct evidence for the existence of intermediate states. Finally, expanding these studies to include complementary experimental systems where ligand-binding is dominated by entropic processes rather than enthalpy should further clarify the relationship between solution thermodynamic parameters and the AFM-measured forces.

Acknowledgements

The authors would like to thank J.N. Israelachvili for helpful discussions. J.Y.W. is grateful for support from a NIH NRSA postdoctoral fellowship (GM17876). V.T.M is supported by the NIH (1 R29 GM55611-01).

References

[1] Creighton TE. Proteins. 2nd ed. New York: WH Freeman and Company, 1993.
[2] Fersht A. Enzyme structure and mechanism. 2nd ed. New York: WH Freeman and Company, 1985.
[3] Helm C, Knoll W, Israelachvili JN. Proc Natl Acad Sci USA 1991;88:8169–73.
[4] Lee GU, Kidwell DA, Colton RJ. Langmuir 1994;10:354–61.
[5] Moy VT, Florin E-L, Gaub HE. Colloids Surfaces 1994;93:343–8.
[6] Florin E-L, Moy VT, Gaub HE. Science 1994;264:415–7.
[7] Pierce M, Stuart J, Pungor A, Dryden P, Hlady V. Langmuir 1994;10:3217–21.
[8] Chilkoti A, Boland T, Ratner BD, Stayton PS. Biophys J 1995;69:2125–30.
[9] Allen S, Davies J, Dawkes AC, Davies MC, Edwards JC, Parker MC, et al. FEBS Lett 1996;390:161–4.
[10] Green NM. Adv Prot Chem 1975;29:85–133.
[11] Weber PC, Ohlendorf DH, Wendoloski JJ, Salemme FR. Science 1989;243:85–8.
[12] Hendrickson WA, Pähler A, Smith JL, Satow Y, Merritt EA, Phizackerley RP. Proc Natl Acad Sci USA 1989;86:2190–4.
[13] Livnah O, Bayer EA, Wilchek M, Sussman JL. Proc Natl Acad Sci USA 1993;90:5076–80.
[14] Sano T, Pandori MW, Smith CL, Cantor CR. In: Uhlén M, Hornes E, Olsvik Ø, editors. Advances in Biomagnetic Separation. Natick, MA: Eaton, 1994:21–9.

[15] Israelachvili JN. Intermolecular and surface forces. 2nd ed. London: Academic Press, 1992.
[16] Gilson MK, Straatsma TP, McCammon JA, Ripoll DR, Faerman CH, Axelsen PH, et al. Science 1994;263:1276–8.
[17] Leckband DE, Schmitt FJ, Israelachvili JN, Knoll W. Biochemistry 1994;33:4611–24.
[18] Hinterdorfer P, Baumgartner W, Gruber HJ, Schilcher K, Schindler H. Proc Natl Acad Sci USA 1996;93:3477–81.
[19] Lee GU, Chrisey LA, Colton RJ. Science 1994;266:771–3.
[20] Dammer U, Popescu O, Wagner P, Anselmetti D, Güntherodt H-J, Misevic GN. Science 1995;267:1173–5.
[21] Ludwig M, Dettmann W, Gaub HE. Biophys J 1997;72:445–8.
[22] Leckband DE, Israelachvili JN, Schmitt FJ, Knoll W. Science 1992;255:1419–21.
[23] Binnig G, Rohrer H. Rev Mod Phys 1987;59:615–25.
[24] Frommer J. Angew Chem Int Ed Engl 1992;31:1265–82.
[25] Evans E, Berk D, Leung A. Biophys J 1991;59:838–48.
[26] Evans E, Ritchie K, Merkel R. Biophys J 1995;68:2580–7.
[27] Stout AL, Webb WW. Meth Cell Biol 1998;55:99–116.
[28] Wang N, Bulter JP, Ingber PE. Science 1993;260:1124–7.
[29] Kuo SC, Lauffenburger DA. Biophys J 1993;65:2191–200.
[30] Israelachvili JN, McGuiggan PM. J Mater Res 1990;5:2223–31.
[31] Darst SA, Ahlers M, Meller P, Kubalek EW, Blankenburg R, Ribi HO, et al. Biophys J 1991;59:387–96.
[32] Weisenhorn AL, Schmitt FJ, Knoll W, Hansma PK. Ultramicroscopy 1992;42–44(Part B):1125–32.
[33] Wong JY, Kuhl TL, Israelachvili JN, Mullah N, Zalipsky S. Science 1997;275:820–2.
[34] Allen TM, Brandeis E, Hansen CB, Kao GY, Zalipsky S. Biochim Biophys Acta 1995;1237:99–108.
[35] Kuhl TL, Leckband DE, Lasic DD, Israelachvili JN. Biophys J 1994;66:1479–88.
[36] Pethica JB, Oliver WC. Physica Scripta 1987;T19:61–6.
[37] Burnham NA, Colton RJ, Pollock HM. J Vac Soc Technol 1991;A9:2548–56.
[38] Hoh JH, Cleveland JP, Prater CB, Revel JP, Hansma PK. J Am Chem Soc 1992;114:4917–8.
[39] Moy VT, Florin E-L, Gaub HE. Science 1994;266:257–9.
[40] Weber PC, Wendoloski JJ, Pantoliano MW, Salemme FR. J Am Chem Soc 1992;114:3197–200.
[41] Chilkoti A, Stayton PS. J Am Chem Soc 1995;117:10622–8.
[42] Chilkoti A, Tan PH, Stayton PS. Proc Natl Acad Sci USA 1995;92:17544–8.
[43] Miyamoto S, Kollman PA. Proteins 1993;16:226–45.
[44] Miyamoto S, Kollman PA. Proc Natl Acad Sci USA 1993;90:8402–6.
[45] Spolar RS, Record Jr MT. Science 1994;263:777–84.
[46] Vajda S, Weng Z, Rosenfeld R, DeLisi C. Biochemistry 1994;33:13977–88.
[47] Leckband D, Muller W, Schmitt FJ, Ringsdorf H. Biophys J 1995;69:1162–9.
[48] Bell GI. Science 1978;200:618–27.
[49] Dembo M, Torney DC, Saxman K, Hammer D. Proc R Soc Lond Ser B 1988;234:55–83.
[50] Evans E, Ritchie K. Biophys J 1997;72:1541–55.
[51] Hänggi P, Talkner P, Borkovec M. Rev Mod Phys 1990;62:251–341.
[52] Grubmüller H, Heymann B, Tavan P. Science 1996;271:997–9.
[53] Izrailev S, Stepaniants S, Balsera M, Oono Y, Schulten K. Biophys J 1997;72:1568–81.